

14

NPS67-80-006

LEVEL II

②

NAVAL POSTGRADUATE SCHOOL
Monterey, California

AD A092135



T. F. McFillin

PTIC
JUL 21 1980
E

AN EXPERIMENTAL INVESTIGATION OF THE DUAL CHAMBER
ROCKET MOTOR.

J. F. McFillin, Jr. / S. T. Van Brocklin
J. E. Beakley / D. W. Netzer

July 1980

Approved for public release; distribution unlimited.

Prepared for:
Naval Weapons Center
China Lake, CA

81 11 24 085

NAVAL POSTGRADUATE SCHOOL

Monterey, California


Rear Admiral J. J. Ekelund
Superintendent

Jack R. Borsting
Provost

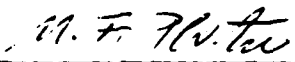
The work reported herein was supported by the Naval Weapons Center,
China Lake, CA., under contract N6053078WR30023.

Reproduction of all or part of this report is authorized.


This report was prepared by:


D. W. NETZER
Associate Professor of Aeronautics

Reviewed by:


M. F. PLATZER, Chairman
Department of Aeronautics

Released as a
Technical Report by:


W. M. TOLLES
Dean of Research

UNCLASSIFIED

SECURITY CLASSIFICATION OF THIS PAGE (When Data Entered)

REPORT DOCUMENTATION PAGE		READ INSTRUCTIONS BEFORE COMPLETING FORM
1. REPORT NUMBER NPS67-80-006	2. GOVT ACCESSION NO. AD-A092	3. RECIPIENT'S CATALOG NUMBER 136
4. TITLE (and Subtitle) AN EXPERIMENTAL INVESTIGATION OF THE DUAL CHAMBER ROCKET MOTOR	5. TYPE OF REPORT & PERIOD COVERED FINAL	
	6. PERFORMING ORG. REPORT NUMBER	
7. AUTHOR(s) J. F. McFillin, Jr., S. T. Van Brocklin, J. E. Beakley, D. W. Netzer	8. CONTRACT OR GRANT NUMBER(s) N6053078WR30023	
9. PERFORMING ORGANIZATION NAME AND ADDRESS NAVAL POSTGRADUATE SCHOOL MONTEREY, CA 93940	10. PROGRAM ELEMENT, PROJECT, TASK AREA & WORK UNIT NUMBERS	
11. CONTROLLING OFFICE NAME AND ADDRESS NAVAL WEAPONS CENTER CHINA LAKE, CA 93555	12. REPORT DATE July 1980	
	13. NUMBER OF PAGES 47	
14. MONITORING AGENCY NAME & ADDRESS (if different from Controlling Office)	15. SECURITY CLASS. (of this report) UNCLASSIFIED	
	15a. DECLASSIFICATION/DOWNGRADING SCHEDULE	
16. DISTRIBUTION STATEMENT (of this Report) Approved for public release; distribution unlimited.		
17. DISTRIBUTION STATEMENT (of the abstract entered in Block 20, if different from Report)		
18. SUPPLEMENTARY NOTES		
19. KEY WORDS (Continue on reverse side if necessary and identify by block number) Rocket Dual Chamber Experimental		
20. ABSTRACT (Continue on reverse side if necessary and identify by block number) An experimental investigation was conducted to further determine the operating characteristics of the dual chamber rocket motor. Axisymmetric and two-dimensional apparatuses were used with air flow to simulate the actual flow. Without special design considerations the sustainer exhaust was found to always shockdown within the booster cavity except for very short booster lengths. Thrust was found to be insensitive to booster cavity length. With nozzle throat area ratios and booster diameters sized		

DD FORM 1 JAN 73 1473

EDITION OF 1 NOV 65 IS OBSOLETE
S/N 0102-014-6601

UNCLASSIFIED

SECURITY CLASSIFICATION OF THIS PAGE (When Data Entered)

UNCLASSIFIED

properly supersonic flow could be maintained within the booster cavity. Practical designs for actual motors appear quite feasible, especially for a nozzleless booster.

Accession For	
NTIS GRA&I	<input checked="checked" type="checkbox"/>
DDC TAB	<input type="checkbox"/>
Unannounced	<input type="checkbox"/>
Justification	
By	
Distribution/	
Availability Codes	
Dist.	Avail and/or special
A	

UNCLASSIFIED

TABLE OF CONTENTS

<u>SECTION</u>		<u>PAGE NO.</u>
I	INTRODUCTION	1
II	SCHLIEREN STUDY OF SHOCKDOWN MODE OF OPERATION . . .	7
	A. Description of Apparatus and Test Conditions . .	7
	B. Results and Discussion	9
III	SUPERSONIC FLOW IN BOOSTER CAVITY	12
	A. Introduction	12
	B. Description of Apparatus and Test Conditions . .	13
	1. Axisymmetric Apparatus	13
	2. 2-D Schlieren Apparatus	15
	C. Results and Discussion	15
IV	TANDEM RAMJET COMBUSTOR FLOW WITH BOOSTER BLAST-TUBE REMOVED	19
	A. Introduction and Description of Apparatus . . .	19
	B. Results and Discussion	19
V	CONCLUSIONS	21
	LIST OF REFERENCES	22
	INITIAL DISTRIBUTION LIST	44

LIST OF FIGURES

PAGE NO.

1. Schematic of 2-D Schlieren Apparatus for Shockdown Mode of Operation	23
2. Schlieren Photograph, Test B1, Converging Nozzle, $L_B = 2.68$ in.	24
3. Schlieren Photograph, Test B2, Converging Nozzle, $L_B = 5.68$ in.	24
4. Schlieren Photograph, Test B3, Converging Nozzle, $L_B = 8.68$ in.	25
5. Schlieren Photograph, Test B4, Converging-Diverging Nozzle, $L_B = 2.55$ in.	26
6. Schlieren Photograph, Test B5, Converging-Diverging Nozzle, $L_B = 5.55$ in.	26
7. Schlieren Photograph, Test B6, Converging-Diverging Nozzle, $L_B = 8.55$ in.	27
8. Schlieren Photograph, Test C1, Converging Nozzle, $L_B = 2.68$ in.	28
9. Schlieren Photograph, Test C2, Converging Nozzle $L_B = 5.68$ in.	28
10. Schlieren Photograph, Test C3, Converging Nozzle $L_B = 8.68$ in.	29
11. Schlieren Photograph, Test C4, Converging-Diverging Nozzle, $L_B = 2.46$ in.	29
12. Schlieren Photograph, Test C5, Converging-Diverging Nozzle, $L_B = 5.46$ in.	30
13. Schlieren Photograph, Test C6, Converging-Diverging Nozzle, $L_B = 8.46$ in.	30
14. Variation of Booster Cavity Pressure with Booster Length, 2-D	31
15. Theoretical Area Ratios Required for Supersonic Flow in Booster Motor	32

	<u>PAGE NO.</u>
16. Schematic of Dual Chamber Motor-- Supersonic Flow in Booster Cavity	33
17. Schematic of 2-D Schlieren Apparatus - Supersonic Flow in Booster Cavity	34
18. Thrust Obtained for Motor with Minimum Theoretically Required Area Ratios	35
19. Thrust Obtained with Sustainer Nozzle Truncation . . .	36
20. Thrust Obtained with Converging Sustainer Nozzle and Nozzleless Booster	37
21. Thrust Variations with Sustainer Nozzle Area Ratios . .	38
22. Schlieren Photographs of Supersonic Flow in Booster Chamber	39
23. Schematic of Tandem Ramjet Configuration	40
24. Tandem Ramjet - Forward Section	41
25. Tandem Ramjet - Nozzle	42
26. Thrust Variations with Booster Motor Pressure- Tandem Ramjet	43

LIST OF TABLES

	<u>PAGE NO.</u>
I. Summary of 2-D Schlieren Configurations for Shockdown Mode of Operation	8
II. Summary of 2-D Schlieren Tests in Shockdown Mode of Operation	11
III. Test Conditions for Supersonic Flow in Axisymmetric Booster Cavity	14
IV. Test Conditions for Supersonic Flow in 2-D Schlieren Apparatus	15

TABLE OF SYMBOLS

A	Area
C_F	Thrust Coefficient
d	Diameter
F	Thrust
h	Height
L	Length
p	Static Pressure
P_o	Stagnation Pressure
γ	Specific Heat Ratio
λ	Nozzle Divergence Loss Factor

Subscripts:

a	Ambient Conditions
B,b	Booster
e	Nozzle Exhaust
N	Nozzle
s	Sustainer
SD	Shockdown
SS	Supersonic Flow

Superscripts:

*	Nozzle Throat Conditions
---	--------------------------

I. INTRODUCTION

Tactical missiles most often have utilized solid fuel rockets for their ease of handling and storage, and their light weight. Demands for higher performance have necessitated new advances in propellants and metallurgy, and pressures have steadily risen. New innovations have become necessary in order to improve overall performance for a propulsion system which has become a mature technology.

Various thrust-time behaviors obtained with new grain configuration and nozzle combinations have been utilized in an attempt to optimize performance for design goals. Boost-sustain motors have been used to meet the demand for medium ranged air-launched tactical missiles.

Boost motors utilize high pressures, high burn rates, and thus short burn times to accelerate tactical missiles to their normal operating speeds, and to provide rapid separation from the launch vehicle. This generally has necessitated an internally burning grain and a large nozzle throat area. Sustainer motors, on the other hand, require longer burn times and operating pressures determined by the desired boost-sustain thrust ratio. Current demands are for thrust ratios up to 20:1. A particular problem occurs when large thrust ratios are required for the boost-sustain motor. If both modes of operation use the same large boost nozzle, then the sustainer would necessarily operate at very low pressures with often unacceptably low burning rates. To obtain adequate pressures and flow rates under these conditions often requires internally burning grains with correspondingly shorter burn times.

Several possible alternatives are available. In principle, the burning rate of the sustainer motor propellant could be increased enough to allow the use of an end burning grain with small surface area. In practice, however, high burning rates are difficult to obtain at low pressures. Separate boost and sustain motors could be employed with the booster ejected after burnout. This is often done on ground/ship launched missiles, but this would present difficulties for air launched systems which usually utilize one set of aft mounted fins for trajectory control.

Another alternative is the variable area nozzle, which requires some form of actuation. This, by itself, leads to increased complexity, weight and expense, not to mention the technical difficulties associated with the high temperatures involved. New technology may permit this concept in the future.

The dual chamber concept involves *some interesting design considerations*. A typical design might incorporate a booster cavity which is nearly fifty sustainer exhaust nozzle diameters in length. From available literature (Refs. 1, 2, 3), free jets have been observed to shockdown within eight to ten diameters. Little is known about the behavior of confined jets. For long booster cavity lengths the sustainer motor exhaust would enter the booster cavity, shockdown, and merely act as a gas generator for the booster nozzle. This in itself may provide sufficient performance advantages over the conventional (one-nozzle) boost-sustain design. However, if the jet impinges on the booster cavity walls, severe problems could arise from high heat transfer rates. This could adversely affect thrust performance, with the increased need for insulation and weight.

If the sustainer exhaust could be made to pass through the boost cavity without shockdown or only partial shockdown, it may be possible to significantly increase thrust as a result of lower stagnation pressure losses.

Benham and Wirtz (Ref. 4) concluded that preventing shockdown did not appear feasible for the tactical dual-chamber concept. This conclusion was based primarily on observed short shockdown lengths. However, these short shockdown distances might still prove beneficial in the tandem approach to the integral-rocket-ramjet (IRR), where combustor lengths are short and the booster exhaust jet may actually pump ramjet air.

The above concept requires that the sustainer jet pass through the booster nozzle, either freely or just attaching at the nozzle throat. While this may not be practical, other possible means exist for reducing stagnation pressure losses. This involves designing the nozzles and booster cavity such that it operates similar to a blow-down supersonic wind tunnel. In this mode of operation the sustainer exhaust would expand (with minimum or no shocks) to the booster cavity wall and flow supersonically into the booster nozzle.

In order to operate in this manner, particular values of nozzle area ratio, and booster cavity length are required. These requirements may or may not be compatible with particular motor geometry restrictions. To operate in the supersonic mode may also require the sustainer exhaust nozzle to be specially contoured to the booster cavity diameter. This may impose severe weight penalties.

The approximate area ratios required can be determined using one-dimensional theory and assuming that the only losses occur across normal shocks

(Ref. 5). The value of the specific heat ratio will significantly affect the required area ratios.

When calculating the necessary area ratios several operating requirements must be met; (a) the sustainer nozzle throat must be small enough to produce the desired high sustainer chamber pressure, (2) the booster throat area must provide adequate booster pressure and loading fraction, (3) the booster throat pressure during sustain operation must be kept greater than ambient pressure to prevent flow separation and to allow "starting" and (4) the booster cavity length probably should be sufficient to allow the sustainer exhaust to expand to the wall.

Whether or not the above restrictions together with possible nozzle contour requirements will allow a practical system to operate remains to be determined.

Another alternative for the dual-chamber concept employs the ejection of the booster nozzle. Here the sustainer motor may be optimized for expansion to atmospheric pressure. Thrust is again provided at sustainer pressures commensurate with long burn times using end burning grains. Expansion of the sustainer exhaust to the booster cavity wall could greatly affect base pressure and thereby cause thrust to vary appreciably with altitude.

The purpose of this investigation was to determine the feasibility and practicality of the dual-chamber concept through a systematic investigation of the pertinent design (nozzle shape and size, booster cavity lengths, etc.) and operational (pressure etc.) variables.

An initial experimental investigation using air flow through the dual chamber geometry with a telescoping booster cavity length considered operating characteristics in the sustainer exhaust shock-down mode of operation (Ref. 6). Configuration variables considered were booster and sustainer nozzle throat diameters and area ratios, booster cavity length, and removal of the booster nozzle.

In the shockdown mode of operation it was found that jet shockdown occurred in 8 to 11 jet diameters as it does in free jet conditions. Sustainer nozzle diameter and area ratio did not significantly alter the shockdown length but did alter the rate of subsonic spreading after shockdown (and therefore the length required to obtain full shockdown pressure). For ideal expansion to shockdown pressure of the sustainer exhaust the jet apparently reached the booster cavity wall in approximately 20 jet diameters. This was also evident in the nozzle-off tests. For booster lengths less than 20 jet diameters, jet penetration of the booster nozzle occurred. This resulted in rapidly decreasing booster cavity static pressure with decreasing cavity length while booster throat static pressure and thrust remained constant.

In the above mode of operation thrust was insensitive to booster cavity length except for extremely short lengths. The sustainer exhaust generally cleared the booster throat for lengths of 3 to 7 jet diameters. Booster nozzle-off operation resulted in large changes in base pressure (and therefore thrust) and also significant system vibrations when the booster cavity length was sufficient to allow the expanding jet to reach the wall.

The present investigation had several objectives:

- (1) To obtain schlieren data in a two-dimensional apparatus to increase the understanding of the results reported in Ref. 6 for operation with sustainer exhaust shockdown.
- (2) To determine operating characteristics for the booster cavity supersonic flow mode of operation using both the axisymmetric motor and the 2-D schlieren apparatus.
- (3) To briefly evaluate the effect of rocket booster blast tube removal on the flow within the ramjet combustor for a tandem integral-rocket-ramjet design.

II. SCHLIEREN STUDY OF SHOCKDOWN MODE OF OPERATION

A. Description of Apparatus and Test Conditions

The schlieren apparatus was a two-dimensional (2-D) device with glass sides in which the simulated booster cavity length, sustainer nozzle size and booster nozzle size could be varied. A schematic of the apparatus is shown in Fig. 1. Table I summarizes the configurations which were utilized. Configuration A used a converging sustainer nozzle with unchoked flow. The remainder of the configurations had a sustainer throat height of 0.336 in. and operated with choked flow. Configurations B and C used 1.3 in. and 1.681 booster throat heights respectively. Both configurations B and C were tested with a converging sustainer nozzle (underexpanded) and converging-diverging nozzle with expansion to approximately the booster cavity shockdown pressure. Booster cavity lengths had nominal values of 3, 6, 9, and 11 in. For each configuration tested sustainer nozzle stagnation pressure (P_{o_s}) and booster cavity wall static pressures were recorded and a schlieren photograph was obtained.

TABLE 1. Summary of 2-D Schlieren Configurations for Shockdown Mode of Operation

DESIG- NATION	NOZZLE [†] CONFIG- URATION	h_s^* (in)	h_{e_s} (in)	h_B^* (in)	A_B^*/A_s^*	A_B/A_s^*	L_B (in)
A	C (unchoked)	.75	.75	1.3	1.73	5.33	10.75, 7.75
B-1	C	.336	.336	1.3	3.87	11.9	8.68, 5.68, 2.68
B-2	C-D	.336	.404	1.3	3.87	11.9	8.55, 5.55, 2.55
C-1	C	.336	.336	1.681	5.0	11.9	8.68, 5.68, 2.68
C-2	C-D	.336	.453	1.681	5.0	11.9	8.46, 5.46, 2.46

[†] C = converging

C-D = converging-diverging

B. Results and Discussion

A summary of the test results are presented in Table II with corresponding Schlieren photographs in Figures 2 through 13. For those tests in which the sustainer exhaust jet did not penetrate the booster nozzle a sketch of the 'window print' (from small amounts of water and oil in the air) is also presented with the schlieren photograph. Fig. 14 presents the fraction of shockdown pressure obtained in the booster cavity as a function of booster cavity length expressed in sustainer nozzle exit heights. Also shown are the data obtained with the axisymmetric apparatus which are presented in Ref. 6. These latter data are for configuration 1 (Figures 11-13, Ref. 6) which was the closest in operating conditions to the 2-D Schlieren tests. In some tests a small amount of leakage into the booster cavity occurred at the upstream corners.

Results obtained from these tests were:

- (1) The length required for the sustainer exhaust jet to shockdown to subsonic flow was 8-11 nozzle exhaust diameters for all tests conducted. This result was the same as was obtained for axisymmetric flow.
- (2) The jet penetrated the booster throat for booster cavity lengths less than approximately 17 sustainer nozzle exit diameters (16-20 for axisymmetric flow). It also penetrated when a converging-diverging sustainer nozzle was used with the large booster nozzle (run #C6).
- (3) When jet penetration of the booster throat occurred the booster cavity wall static pressures were pumped down in a manner similar to that obtained for axisymmetric flow.

- (4) When booster cavity length was sufficient to prevent jet penetration of the booster throat a normal 2-D jet behavior occurred, i.e., the jet would "flip" to one side and oscillate slightly in position with time. When the jet behaved in this manner (Runs B3, B6, and C3) booster cavity wall static pressure reached the shockdown pressure near the end of the chamber. Wall static pressures generally decreased toward the sustainer exhaust nozzle although some variations occurred. The latter apparently resulted from the jet impingement on one wall and then on the other (see Fig. 7).
- (5) The core of the expanding subsonic portion of the jet never reached the booster cavity wall (except when the whole jet flipped to one side) for the lengths investigated.

TABLE 11. SUMMARY OF 2-D SCHLIEREN TESTS IN SHOCKDOWN MODE OF OPERATION

RUN NO.	DESIG (TABLE 1)	P _{OS} (psia)	BOOSTER CHAMBER LENGTH (in)	BOOSTER CAVITY PRESSURES P _B (psia)								P _e (psia)	P _B max P _{OSD}	P _{OSD} (psia)	SCHLIEREN PHOTO-GRAPH FIG. NO.
				P ₁	P ₂	P ₃	P ₃	P ₄	P ₄	P ₄	P ₅				
A 1	A	86.9	7.75	32.65	31.26	-	-	44.16	49.76	-	-	-	-	-	-
A 2	A	86.9	10.75	33.34	31.31	-	-	31.50	-	35.88	44.99	-	-	-	-
B 1	B-1	194.7	2.68	-	16.74	19.07	-	-	-	-	-	102.9	0.38	50.3	2
B 2	B-1	194.7	5.68	-	21.03	-	22.57	26.03	-	-	-	102.9	0.52	50.3	3
B 3	B-1	194.8	8.68	-	30.74	-	30.71	-	40.83	51.34	51.34	102.9	1.03	50.3	4
B 4	B-2	194.7	2.55	-	15.08	-	16.91	-	-	-	-	50.3	0.34	50.3	5
B 5	B-2	194.7	5.55	-	19.46	21.19	-	24.08	-	-	-	50.3	0.48	50.3	6
B 6	B-2	194.8	8.55	-	35.63	-	35.88	-	28.76	46.30	46.30	50.3	0.92	50.3	7
C 1	C-1	194.7	2.68	-	15.97	15.06	-	-	-	-	-	102.9	0.39	38.9	8
C 2	C-1	194.6	5.68	-	-	-	15.04	16.70	-	-	-	102.9	0.43	38.9	9
C 3	C-1	194.7	8.68	-	18.38	-	18.62	-	31.51	38.52	38.52	102.9	0.99	38.9	10
C 4	C-2	194.7	2.46	-	19.57	18.45	-	-	-	-	-	38.8	0.47	38.9	11
C 5	C-2	194.6	5.46	-	-	-	18.97	17.25	-	-	-	38.8	0.44	38.9	12
C 6	C-2	194.7	8.46	-	16.15	-	15.40	-	15.97	18.02	18.02	38.8	0.46	38.9	13

III. SUPERSONIC FLOW IN BOOSTER CAVITY

A. Introduction

The primary purpose of this portion of the study was to determine the effects of the sustainer and booster nozzle geometries on the maintenance of supersonic flow within the booster cavity. No attempt was made in this initial study to examine a wide range of booster/sustainer throat area ratios or booster cavity length/diameter ratios. The specific area ratios and flow rates selected were chosen to be as near a "practical design" as possible within the air flow rate/pressure limitations of an existing blow-down air supply system. Both axisymmetric and 2-D schlieren tests were conducted.

The booster/sustainer nozzle throat area ratio required to maintain supersonic flow in the booster cavity depends upon the sustainer nozzle area ratio and the stagnation pressure losses (shocks, wall friction, etc.) throughout the apparatus. In addition, sufficiently low ambient pressure (or sufficiently high sustainer pressure) must be present. The minimum area ratio requirements are readily calculated (pp. 394-399, Ref. 5). Figure 15 presents the minimum required area ratios for $\gamma = 1.4$ and 1.2. Increasing losses (oblique shocks, longer booster cavity, etc.) would increase the required area ratios. In an actual dual-chamber design A_B^*/A_S^* would be primarily dictated by motor operating requirements (thrust ratios, etc.) and available propellant ballistic properties. In this investigation only air flow was utilized. Figure 15 shows that for actual propellant exhaust products (γ closer to 1.2) and a specified sustainer throat diameter, larger booster cavity and booster throat

diameters are required. This also results in a larger required booster nozzle contraction ratio. Thus, actual motor designs would have more favorable geometry for high propellant loading than those required in this investigation which used air flow.

B. Description of Apparatus and Test Condition

1. Axisymmetric Apparatus

The same air supply system was employed as reported in Ref. 6. This system was limited to approximately 2.5 lbm/sec. The same sustainer motor simulator was also employed. However, in order to reduce the booster cavity Mach number to 3.0 its diameter was reduced to 1.0 inch. This reduction was required in order to be able to "start" and maintain supersonic flow within the booster cavity while remaining within the flow rate limitations (i.e., $p_B^* > p_a$ and $p_{e_B} > 0.5 p_a$). Figure 16 is a schematic of the apparatus. A 15° half-angle cone was installed to allow the sustainer nozzle flow to expand smoothly to the booster cavity diameter. This nozzle was truncated for subsequent tests until only a converging nozzle remained. Table III summarizes the geometric variations and test conditions employed for each configuration investigated. Equations employed for calculating the theoretically obtainable thrust with shockdown and full supersonic flow are also presented in Table III.

TABLE III. TEST CONDITIONS FOR SUPERSONIC FLOW IN AXISYMMETRIC BOOSTER CAVITY

CONFIG.	$d_B^*(in)$	$d_s^*(in)$	$d_{e_s}(in)$	A_B^*/A_s^*	$(A_e/A^*)_B$	$(A_e/A^*)_s$	A_{eB}/A_s^*	P_{eB}/P_{O_s}	$(P_e/P_O)_B$	$P_{O_s} (psia)$
1	.848	.486	1.00	3.045	1.683	4.234	5.123	0.02022	.1285	305,487
2	.90	.486	1.00	3.429	1.494	4.234	5.123	0.02022	.1615	495,585
3	.90	.486	.872	3.429	1.494	3.219	5.123	0.02022	.1615	302,410, 486, 619, 708
4	.90	.486	.667	3.429	1.494	1.884	5.123	0.02022	.1615	328,407, 506, 606, 711
5	.90	.486	.486	3.429	1.494	1.00	5.123	0.02022	.1615	299, 390, 499, 615, 711
6	1.00	.486	.486	4.234	1.210	1.00	5.123	0.02022	.2542	197,297, 392,493, 578,685

$$F_{SD} = \lambda C_F P_{O_s} A_B^* = \lambda C_F \left(\frac{A_s^*}{A_B^*} \right) P_{O_s} A_B^*$$

$$C_F = C_F \left(\gamma, \frac{P_e}{P_{O_s}}, \left(\frac{A_e}{A^*} \right)_B \right)$$

$$F_{SS} = C_F P_{O_s} A_s^*$$

$$C_F = C_F \left(\gamma, \frac{P_{eB}}{P_{O_s}}, \frac{A_{eB}}{A_s^*} \right)$$

Configuration 1 had the theoretically (Fig. 15) required area ratios. The booster throat area was increased by 13% for configurations 2 through 5 and by 39% for configuration 6.

2. 2-D Schlieren Apparatus

The apparatus employed was the same as presented above in Section IIA. However, to limit booster cavity Mach number (2.52) and to insure that full supersonic flow could be attained ($p_B^* > p_a$) the cavity height was reduced to 2.0 in. A schematic of the test configuration is shown in Fig. 17. Test conditions are presented in Table IV. Configuration 1 employed the theoretically required (Fig. 15) area ratios. For configuration 2 the booster throat area was increased by 17%.

TABLE IV. Test Conditions for Supersonic Flow in 2-D Schlieren Apparatus

<u>CONFIG.</u>	$h_s^*(\text{in.})$	$h_B^*(\text{in})$	A_B/A_s^*	A_B^*/A_s^*	A_B/A_B^*
1	.75	1.53	2.67	2.036	1.31
2	.75	1.79	2.67	2.386	1.12

C. Results and Discussion

Fig. 18 presents measured thrust as a function of sustainer pressure for Configuration 1 with axisymmetric flow (Table III). Also shown on the figure are the theoretical values for (a) thrust with full supersonic flow and with shockdown, (b) booster cavity shockdown pressure, and (c) booster cavity pressure for full supersonic flow with no losses. Measured values of booster cavity pressure (p_1 and p_2 : see Fig. 16) are also presented. p_2 was nearest the booster nozzle. The pressure and thrust results indicate that full shockdown occurred with the theoretically required area ratios.

Fig. 19 presents similar results for Configurations 2 through 5 (Table III). As the sustainer nozzle was truncated in increments the booster cavity flow transitioned from nearly shock free supersonic flow to a full shockdown behavior. In configuration 2, small increases in booster cavity static pressure above that for full supersonic flow would result from the shock formed at the junction of the sustainer nozzle cone and the booster cavity wall. Reflection of this shock further downstream would further raise the static pressure (note that $p_2 > p_1$). The shock plus frictional losses were not great enough to prevent "starting" of the supersonic flow through the enlarged (13%) booster nozzle throat.

As the sustainer nozzle was truncated the shocks increased in strength, increasing the booster cavity static pressure and reducing the thrust. Configuration 4 apparently maintained supersonic flow (low p_1 and p_2) in the booster cavity but the shock losses reduced the thrust to near theoretical shockdown values. When the sustainer nozzle was convergent, full shockdown conditions were apparently obtained. In this case the shock losses were apparently too great to allow "starting" of the flow through the booster throat.

For Configuration 6 the booster throat area was again increased (39% greater than theoretical and 23% greater than Configurations 2 through 5) to allow for "starting" with the larger shock losses obtained with the converging sustainer nozzle. Fig. 20 shows that supersonic flow was again attained in the booster cavity, although with losses large enough to significantly reduce the thrust.

The thrust obtained with $P_{O_s} = 600$ psia and A_B^* 13% larger than theoretical is shown in Fig. 21 as a function of sustainer nozzle area ratio. Data from the previous figures have been used by "correcting" the "near 600 psia" runs to 600 psia.

Configuration 1 (Table IV) for the 2-D schlieren tests also employed the theoretically required area ratios and also resulted in full shockdown (near normal shock close to sustainer nozzle throat) in the booster cavity. Configuration 2 (with A_B^* increased 17% above the theoretically required) resulted in supersonic booster cavity flow. Figure 22 presents schlieren photographs obtained with two different sustainer pressures.

These results indicate that full supersonic flow can be obtained in the booster cavity of the dual chamber rocket configuration. Maximizing the obtainable thrust required increasing the area ratio (and therefore weight) of the sustainer nozzle. With a converging sustainer nozzle supersonic flow can be maintained and thrust increased above shockdown values. However, the booster throat area required becomes quite large. A nozzleless booster would probably be required in this case.

The configurations tested in this study were of limited scope. It should be noted that shockdown dual chamber configurations that have been tested to date (Ref. 7) have employed A_B^*/A_S^* values only slightly greater than those used in Configuration 6 (Table III). However, much longer and larger diameter booster cavities have been employed in the actual motors. The larger diameter would result in slightly higher booster cavity Mach numbers (approximately 4.5 with $\gamma = 1.2$) and the longer lengths would increase losses. These changes would require further increases in

the booster nozzle throat area above that theoretically required. Shock impingement on the booster cavity wall may also require local increases in insulation material. However, a nozzleless booster cavity with a Mach number of approximately 3.5 would allow A_B/A_S^* to be as large as approximately 21 ($\gamma = 1.2$) and would have a theoretical booster cavity pressure of 8.5 psia (with $P_{O_S} = 1500$ psia). Shock and friction losses would increase this pressure somewhat, providing a reasonable exhaust pressure at sea level for the supersonic flow.

IV. TANDEM RAMJET COMBUSTOR FLOW WITH BOOSTER BLAST-TUBE REMOVED

A. Introduction and Description of Apparatus

The tandem integral-rocket-ramjet configuration employs a short annular ramjet combustor. The solid rocket booster exhausts through a blast tube which passes down the center of the ramjet combustor. In this configuration booster nozzle and inlet port cover ejections are not required. If the blast tube could be removed a considerable weight savings could be attained. However, the effects of this truncation are not known and are very difficult to predict analytically. The effects will depend upon the specific geometry employed, the booster flow rate, and the flight Mach number (ram air).

The investigation was very limited, being restricted to looking at a scaled-down model of one current tandem design. The purpose of the tests was to determine whether or not the booster exhaust would aspirate or eject air through the ramjet inlets. This would have design implications with regard to shock positions within the ramjet inlet during boost. No attempt was made to have ram air into the inlets and the inlets were simply simulated using four holes drilled normal to the motor centerline.

A schematic of the configuration is shown in Fig. 23 and detailed drawings are presented in Figs. 24 and 25. Small tufts were attached to the ramjet chamber inlet ports for flow visualization purposes.

B. Results and Discussion

The apparatus was mounted on the thrust stand and operated with booster cavity pressure from 500 to 1500 psia. In all tests air was aspirated into the booster cavity as evidenced by the motion of the tufts.

Figure 26 presents the thrust obtained. Also shown for comparison are the values of theoretical thrust for two limiting cases: the booster without the ramjet attached and the thrust obtained if shockdown occurred in the ramjet cavity and no air were aspirated.

The ramjet cavity was only approximately three booster nozzle exit diameters in length. Based upon the results presented in Reference 6 and above for the dual chamber rocket configuration, the booster exhaust probably passed freely through the ramjet nozzle throat before shockdown could occur (in 8 to 10 jet diameters). The ramjet cavity was therefore pumped to less than atmospheric pressures, causing air to aspirate through the four radial inlets.

These results imply that blast tube removal probably would not have large adverse effects on ramjet operation during the boost phase.

V. CONCLUSIONS

- A. Sustainer exhaust shockdown occurs within 8 to 11 jet diameters within the booster cavity as it does in free jet conditions.
- B. Sustainer exhausts begin to penetrate the booster nozzle (for the geometries tested) throat for booster chamber lengths less than approximately 17 jet diameters, resulting in rapid decreases in booster cavity static pressure with decreasing cavity length while thrust remains unaffected.
- C. Sustainer exhaust jets will generally clear the booster throat for booster chamber lengths between 3 and 7 jet diameters.
- D. 2-D schlieren results generally confirmed the behavior found in the axisymmetric apparatus.
- E. Sizing the booster nozzle throat slightly greater than theoretically required allows supersonic flow to be maintained within the booster cavity and results in significant gains in thrust over the shockdown behavior.
- F. Sustainer exhaust nozzle truncation increases shock losses and reduces the obtainable thrust but supersonic flow can be maintained with a converging sustainer nozzle.
- G. Practical designs appear feasible for an actual motor in which supersonic flow is maintained within the booster cavity. Nozzleless boosters would enhance the obtainable performance gains.
- H. Shock impingements on the booster cavity walls may significantly damage insulation and requires investigation in actual motor fringes.

LIST OF REFERENCES

1. Donaldson, C. and Gray, K., "Theoretical and Experimental Investigation of the Compressible Free Mixing of Two Dissimilar Gases," AIAA J., Vol. 4, No. 11, pp. 2017-2025, November 1966.
2. Tufts, L. W. and Smoot, L. D., "A Turbulent Mixing Coefficient Correlation for Coaxial Jets with and without Secondary Flows," J. of Spacecraft and Rockets, Vol. 8, No. 12, pp. 1183-1190, December 1971.
3. Morris, P. J., "Turbulence Measurements in Subsonic and Supersonic Axisymmetric Jets in Parallel Stream," AIAA J., Vol. 14, No. 10, pp. 1468-1475, October 1976.
4. Benham, C. B. and Wirtz, D. P., "Dual-Chamber Performance Analysis," NWC Memorandum to J. Andrews 3245/CBB: CAS, Reg. 3245-40-77, 5 May 1977.
5. Zucrow, M. J. and Hoffman, J. D., Gas Dynamics, Vol. 1, John Wiley and Sons, 1976.
6. McFillin, Jr., J. F. and Netzer, D. W., "An Experimental Investigation of the Dual Chamber Rocket," Naval Postgraduate School Report NPS67-79-001, January 1979.
7. Fling, M., Atchley, R. D., Stokes, B. B., Fry, P., Netzer, D. W., "The Dual Chamber Rocket Motor and Its Advantages in Tactical Propulsion: Analytical Model, Mission Analysis and Demonstration Testing", presented at 1980 JANNAP Propulsion Meeting, Monterey, Ca.

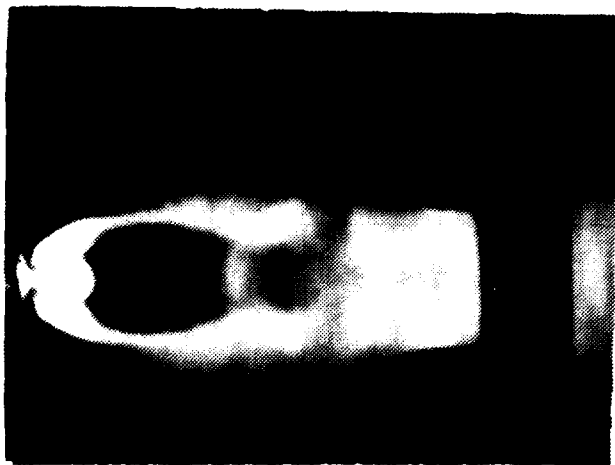


Figure 2. Schlieren Photograph, Test B1
Converging Nozzle, $L_B = 2.68$ in.

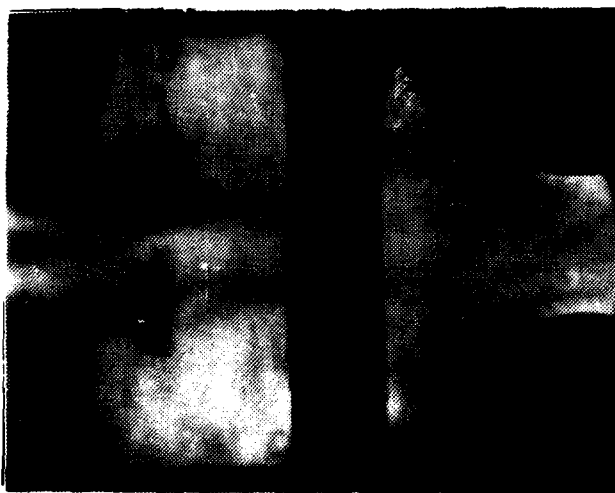


Figure 3. Schlieren Photograph, Test B2
Converging Nozzle, $L_B = 5.68$ in.

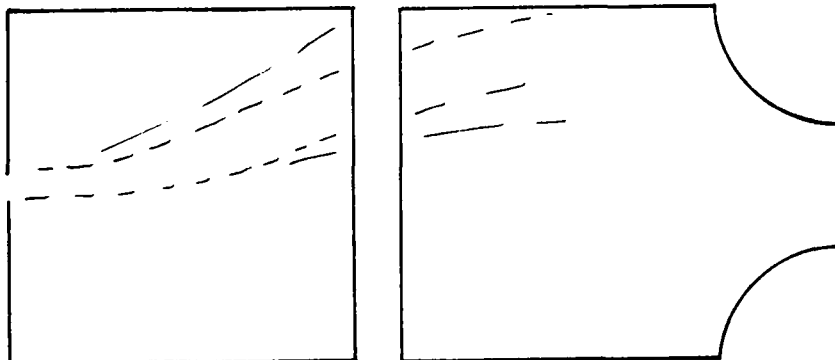


Figure 4. Schlieren Photograph, Test B3, Converging Nozzle, $L_B = 8.68$ in.



Figure 5. Schlieren Photograph, Test B4,
Converging-Diverging Nozzle, $M = 2.55$ in.



Figure 6. Schlieren Photograph, Test B5,
Converging-Diverging Nozzle, $M = 2.55$ in.

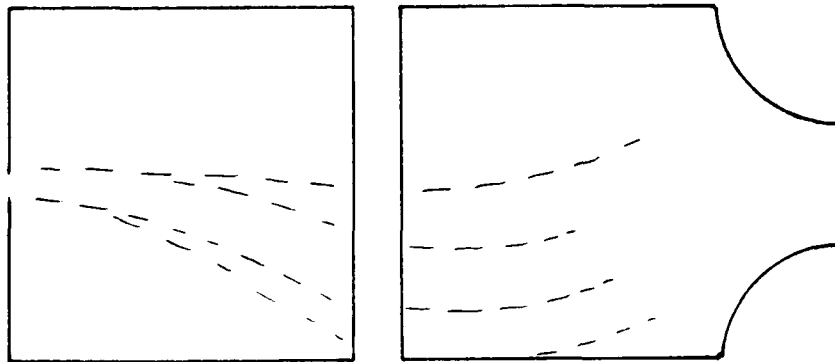
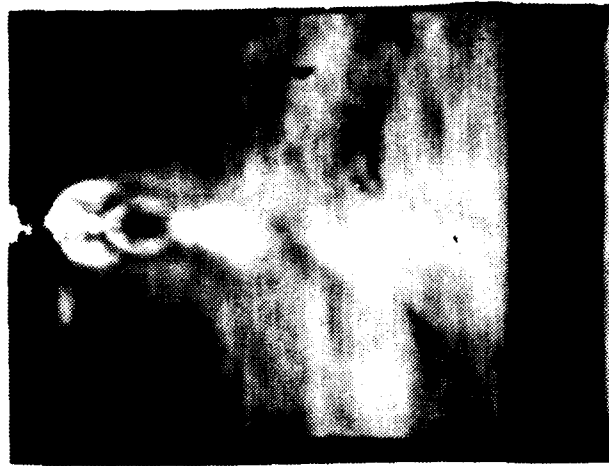


Figure 7. Schlieren Photograph, Test B6,
Converging-Diverging Nozzle, $L_B = 3.55$ in.



Figure 8. Schlieren Photograph, Test C1,
Converging Nozzle, $L_3 = 2.68$ in.



Figure 9. Schlieren Photograph, Test C2,
Converging Nozzle, $L_3 = 2.68$ in.

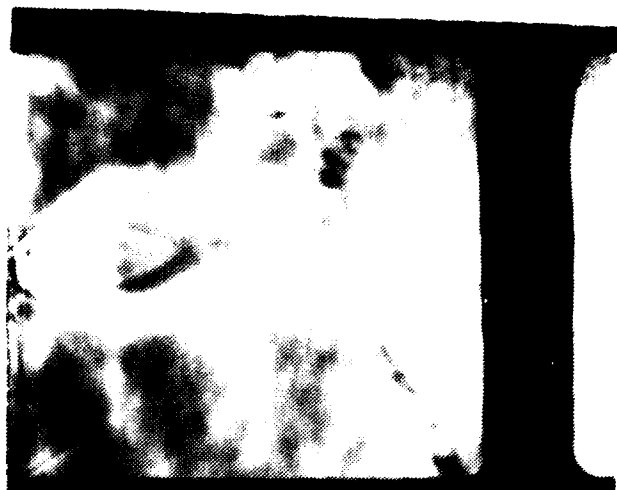


Figure 10. Schlieren Photograph Test C3
Converging Nozzle, $L_L = 8.68$ in.

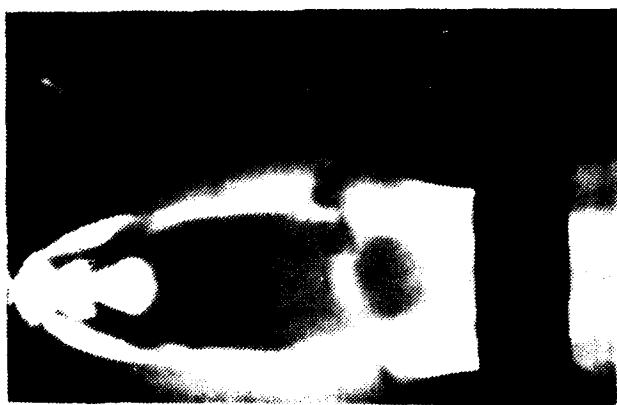


Figure 11. Schlieren Photograph, Test C4
Converging-Diverging Nozzle, $L_B = 2.46$ in.



Figure 12. Schlieren Photograph, Test C5,
Converging-Diverging Nozzle, $L_b = 5.46$ in.



Figure 13. Schlieren Photograph, Test C6,
Converging-Diverging Nozzle, $L_b = 8.46$ in.

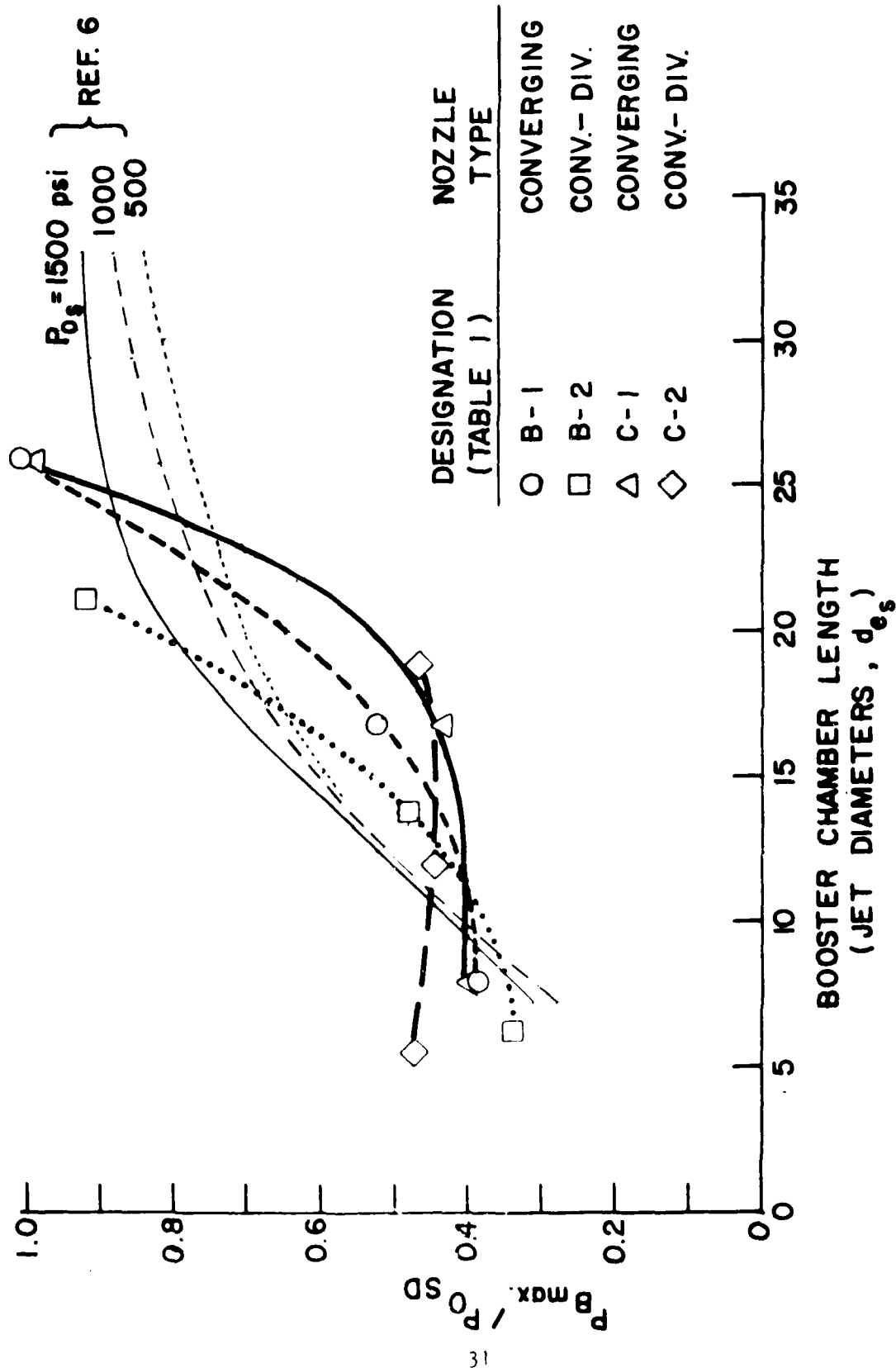
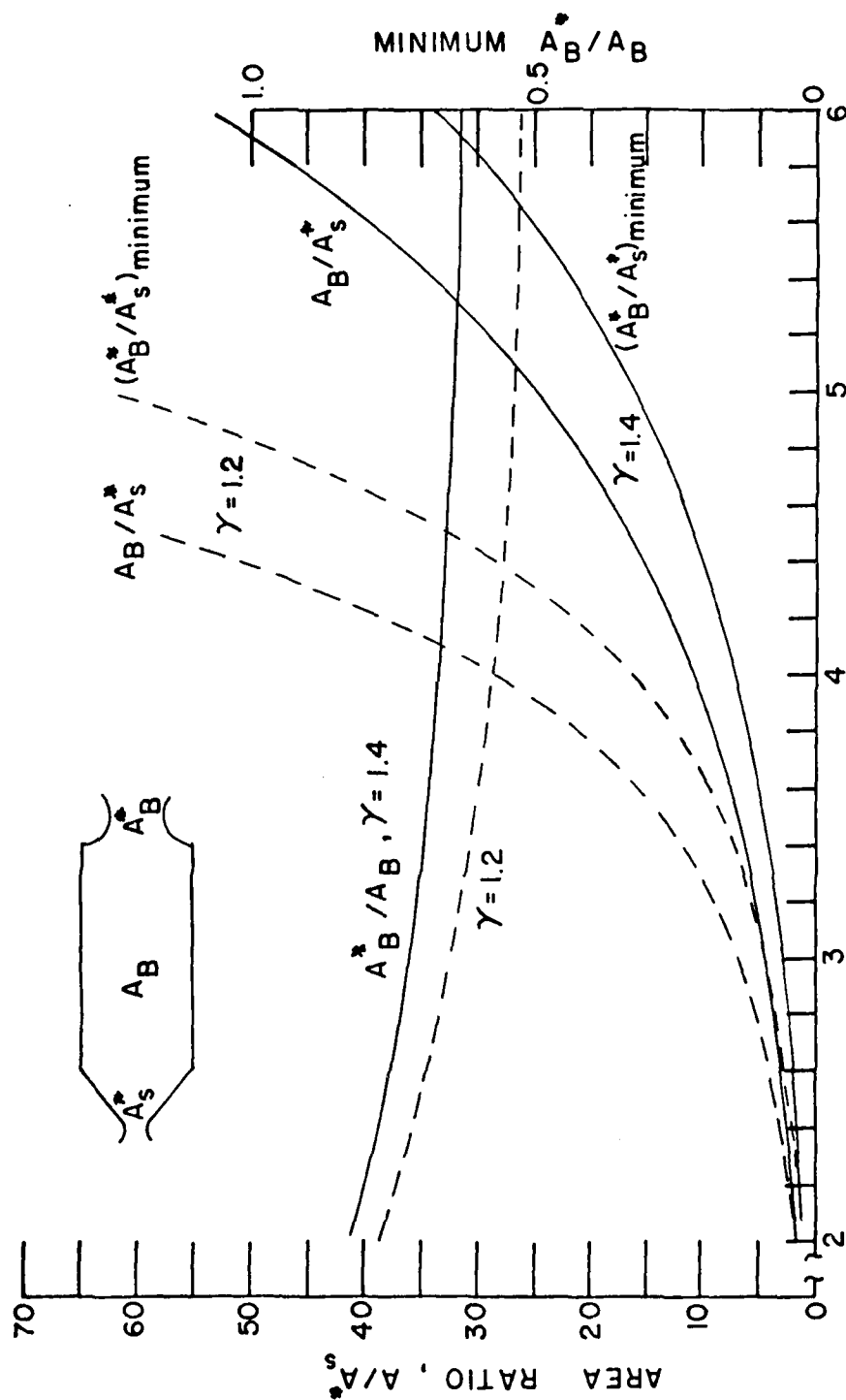


Figure 14. Variation of Booster Cavity Pressure with Booster Length, 2D



BOOSTER CHAMBER MACH NUMBER

Figure 15. Theoretical Area Ratios Required for Supersonic Flow in Booster Motor

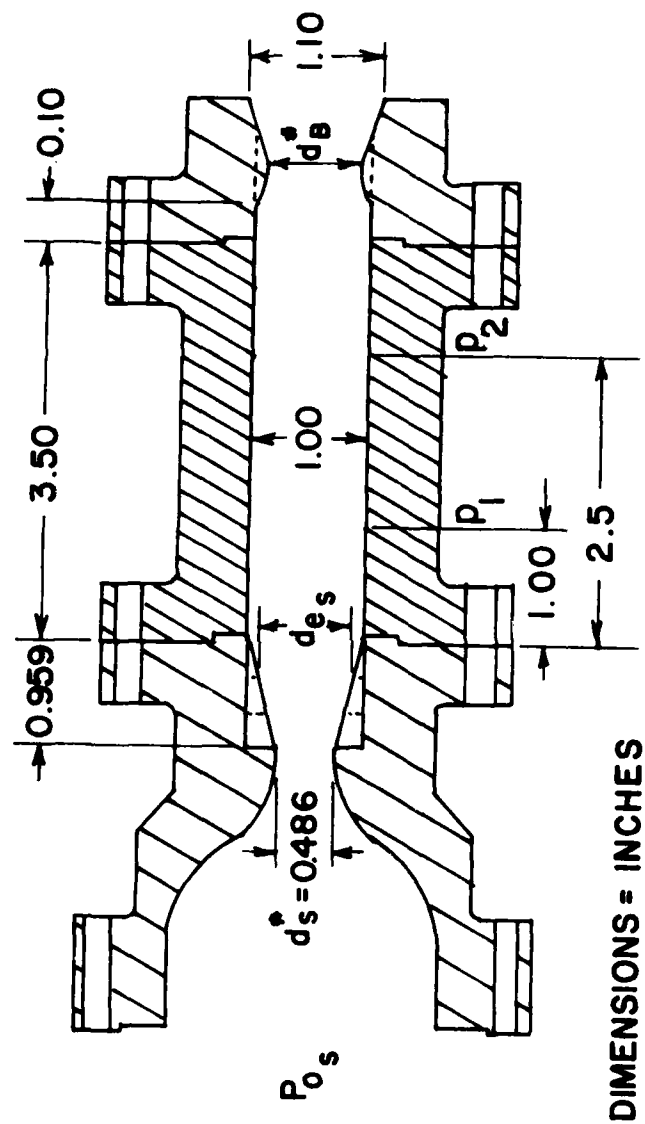


Figure 16. Schematic of Dual Chamber Motor -- Supersonic Flow in Booster Cavity

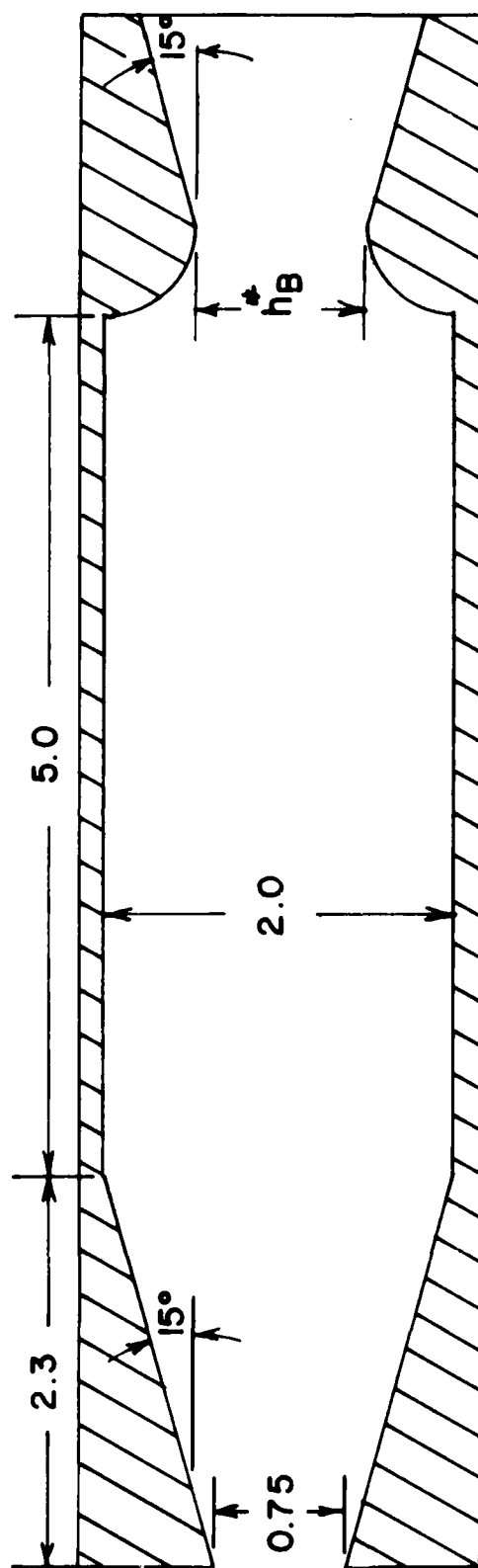
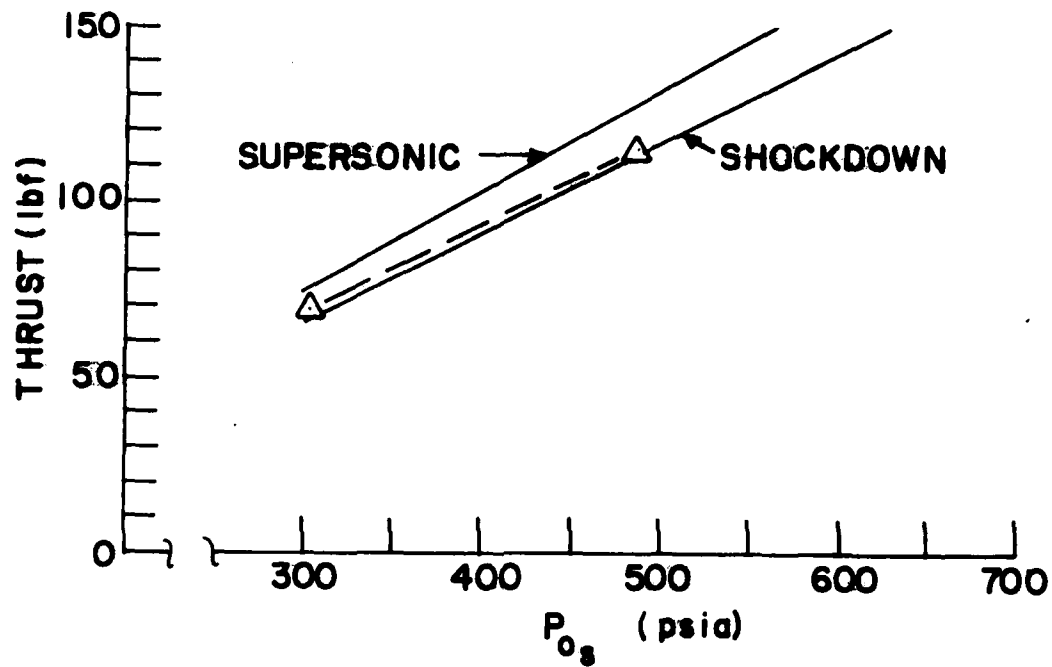
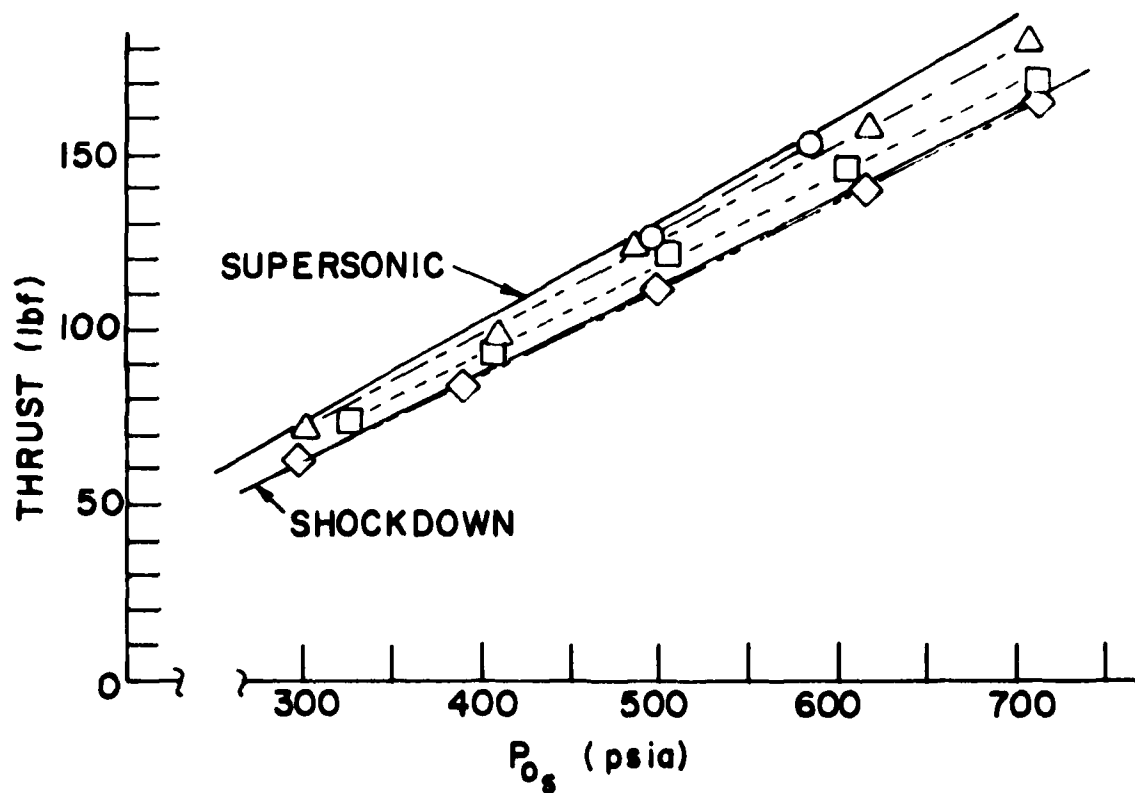


Figure 17. Schematic of 2-D Schlieren Apparatus - Supersonic Flow in Booster Cavity



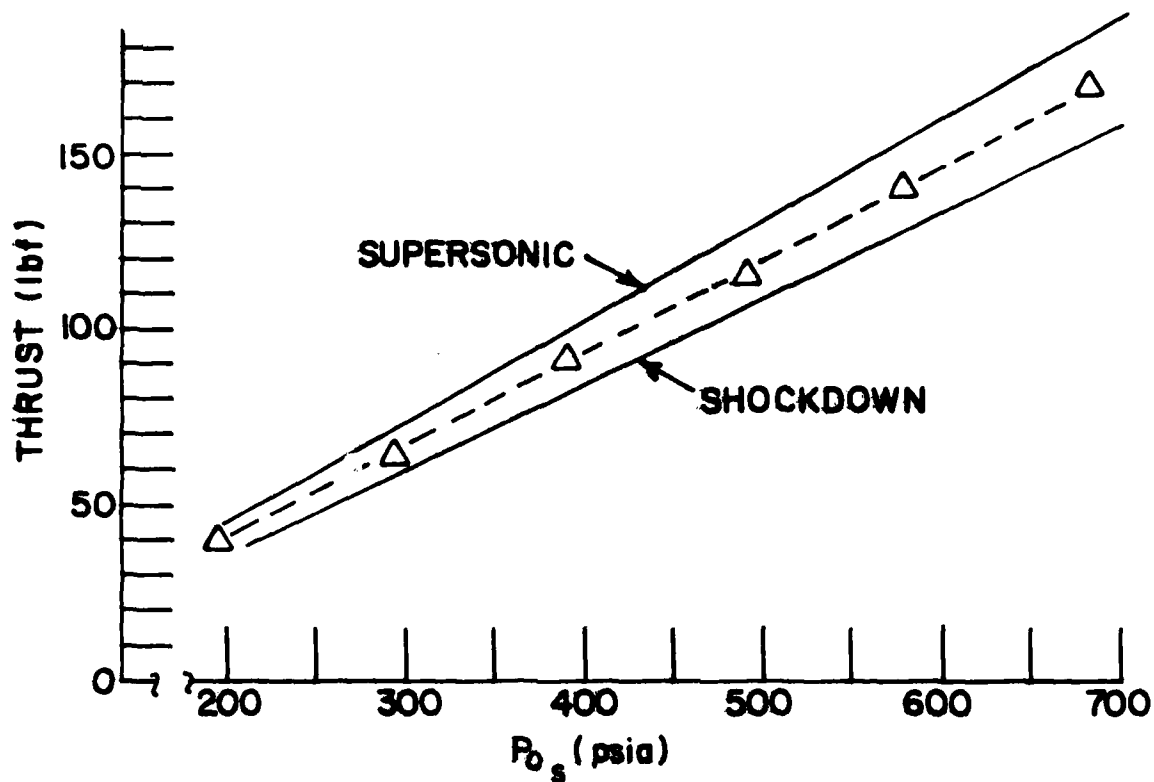
P_{0s} (psia)	$F(lb_f)$	p_1 (psia)	p_2 (psia)	Theoretical	
				$p_{B_{ss}}$	P_{0SD}
305	68	49.0	73.2	8.3	100.2
487	115	80.4	118.9	13.3	160.0

Figure 18. Thrust Obtained for Motor with Minimum Theoretically Required Area Ratios (Config. 1, Table III)



Config. (Table III)	d_{e_s} (in.)	P_{0s} (psia)	F (lbf)	P_1 (psia)	P_2 (psia)	Theoretical $P_{B_{ss}}$ (psia)	P_{0SD} (psia)
2	1.00	495	127	13.5	20.2	13.5	144.3
		585	153	15.9	23.9	15.9	170.6
3	.872	302	72	9.0	12.8	8.2	88.1
		410	99	11.8	15.8	11.2	119.6
		486	125	14.2	20.6	13.2	141.7
		619	158	16.7	25.3	16.9	180.5
		708	181	20.2	30.0	19.3	206.5
4	.667	328	73	10.4	13.6	9.0	95.6
		407	94	12.8	16.9	11.1	118.7
		506	121	15.9	21.0	13.8	147.5
		606	146	18.9	25.0	16.5	176.7
		711	172	22.1	29.2	19.4	207.3
5	.486	299	63	65.9	70.2	8.2	87.2
		390	83	84.8	90.2	10.6	113.7
		499	111	108.5	115.2	13.6	145.5
		615	140	133.9	142.2	16.8	179.3
		711	165	153.3	165.6	19.4	207.3

Figure 19. Thrust Obtained with Sustainer Nozzle Truncation



Config. (Table III)	d_{es} (in.)	P_{os} (psia)	F (lbf)	P_1 (psia)	P_2 (psia)	Theoretical	
						$P_{B_{ss}}$ (psia)	P_{osD} (psia)
6	.486	197	40	12.7	12.2	5.4	46.5
		297	64	19.4	18.5	8.1	70.2
		392	91	25.4	24.3	10.7	92.6
		493	115	31.8	30.4	13.4	116.5
		578	140	38.0	36.1	15.7	136.5
		685	168	44.8	42.8	18.7	161.8

Figure 20. Thrust Obtained with Converging Sustainer Nozzle and Nozzleless Booster

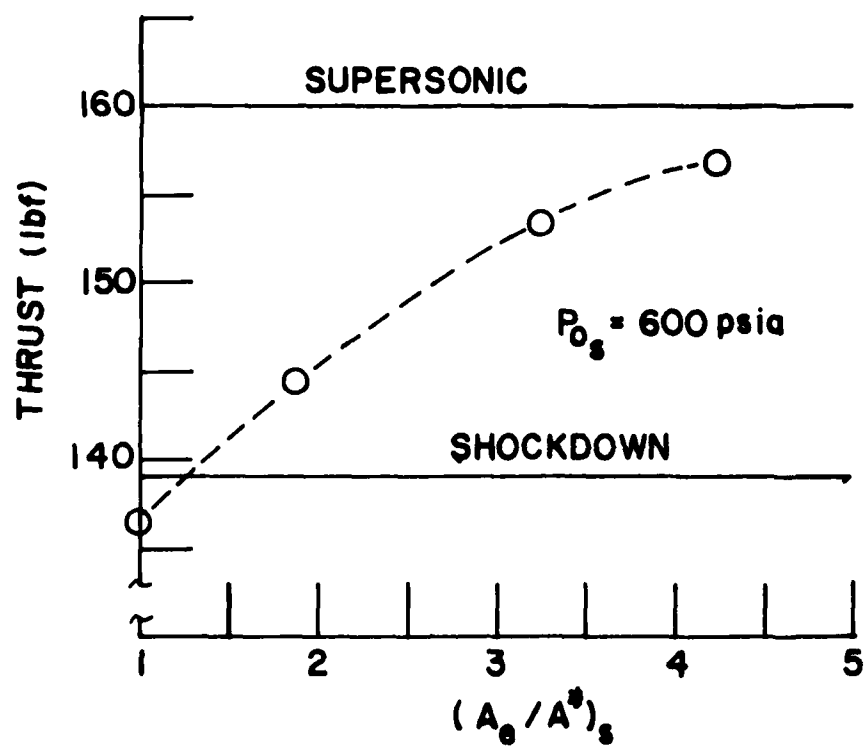
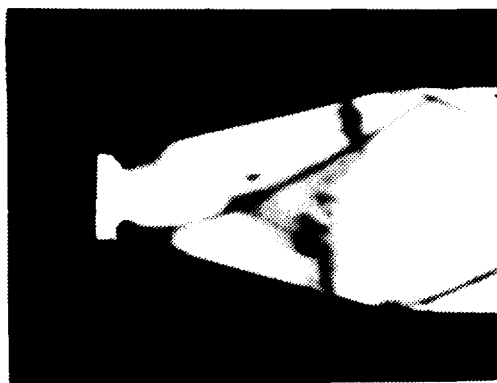
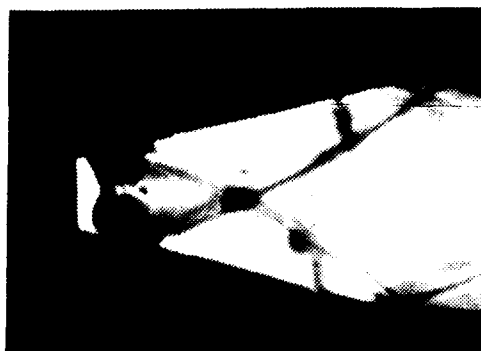


Figure 21. Thrust Variations with Sustainer Nozzle Area Ratios



(a) $P_{0s} = 42$ psia



(b) $P_{0s} = 215$ psia

Figure 22. Schlieren Photographs of Supersonic Flow in Booster Chamber

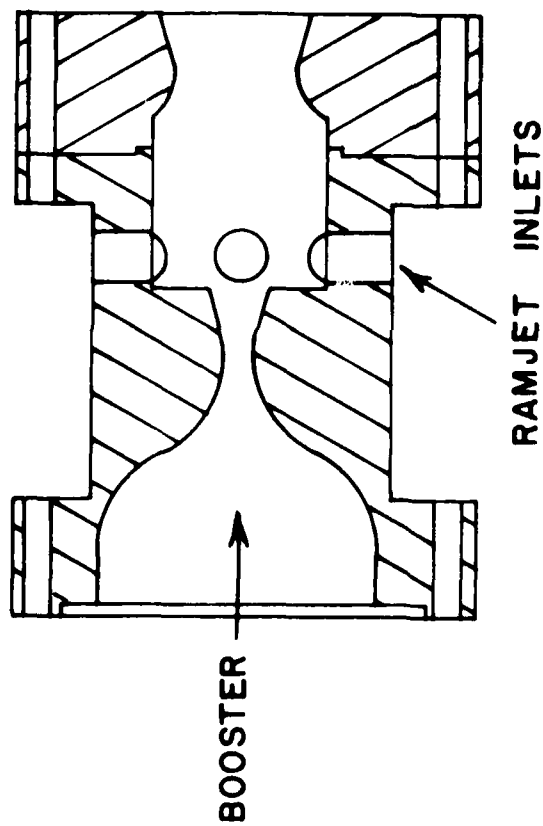


Figure 23. Schematic of Tandem Ramjet Configuration

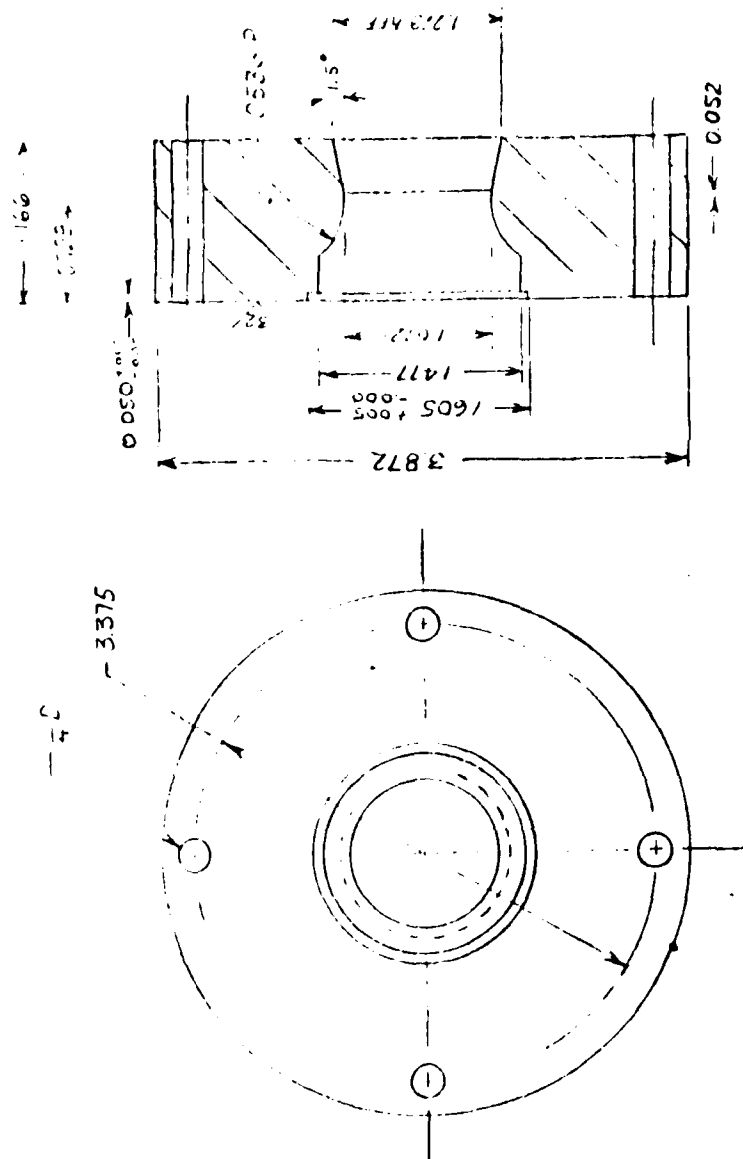


Figure 25. Tandem Ramjet - Nozzle

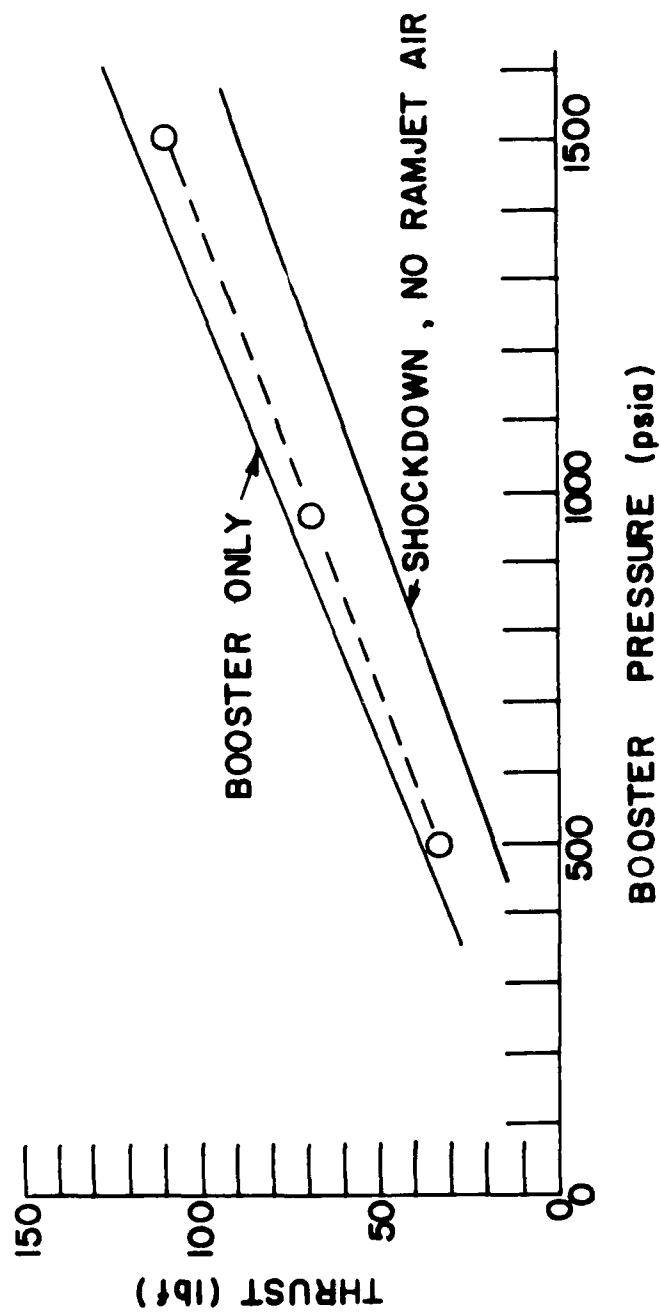


Figure 26. Thrust Variations with Booster Motor Pressure - Tandem Ramjet

INITIAL DISTRIBUTION LIST

	<u>NO. OF COPIES</u>
1. Library Code 0142 Naval Postgraduate School Monterey, CA 93940	2
2. Department of Aeronautics Code 67 Naval Postgraduate School Monterey, CA 93940 M. F. Platzter, Chairman D. W. Netzer	1 12
3. Dean of Research Code 012 Naval Postgraduate School Monterey, CA 93940	1
4. Defense Technical Information Center Cameron Station Alexandria, VA 22314	2
5. Commanding Officer Naval Air Systems Command Department of the Navy Washington, DC 20360 (AIR-03B, 03P2, 30212, 320, 340B, 503, 510B, 5105, 5203C, 5312, 532, 5366)	13
6. Chief of Naval Material Department of the Navy Washington, DC 20360 (MAT-030B, 032, NSP-27, 2731)	4
7. Commanding Officer Naval Sea Systems Command Headquarters Washington, DC 20362 (ATTN: Code 6542D)	1
8. Commanding General Marine Corps Development and Education Command Quantico, VA 22134 (ATTN: Director, Marine Corps Landing Force Development Center)	3

NO. OF COPIES

- | | | |
|-----|---|---|
| 9. | Commander
Air Test & Evaluation Squadron
5-VX-5
Naval Air Facility
China Lake, CA 93555 | 1 |
| 10. | Officer in Charge
Fleet Analysis Center
Naval Weapon Station, Seal B
Corona, CA 91720 | 1 |
| 11. | Commanding Officer
Naval Ammunition Depot
Hawthorne, NV 89415
(Code 05, Robert Dempsey) | 1 |
| 12. | Commanding Officer
Naval Explosive Ordnance Disposal
Facility
Indian Head, MD 20640 | 1 |
| 13. | Commanding Officer
Naval Intelligence Support Center
4301 Suitland Road
Washington, DC 20390
(Attn: 00XA, CDR Jack Darnell) | 1 |
| 14. | Commanding Officer
Naval Ocean Systems Center
San Diego, CA 92152
(ATTN: Code 133) | 1 |
| 15. | Commanding Officer
Naval Ordnance Station
Indian Head, MD 20640
(Attn: Code PM) | 1 |
| 16. | Naval Surface Weapons Center Dahlgren Laboratory
Dahlgren, VA 22448
(Code DG, Attn: C. L. Dettinger) | 2 |
| 17. | Commanding Officer
Naval Surface Weapons Center
White Oak
Silver Spring, MD 20910
(Attn: Code WR) | 1 |

	<u>NO. OF COPIES</u>
18. Commanding Officer Naval Intelligence Support Center Liaison Officer 4301 Suitland Road Washington, DC 20390 (Attn: LNN)	1
19. Commanding Officer Army Armament Material Readiness Command Rock Island, IL 61201 (Attn: DRSAR-LEM)	1
20. Commanding General Army Ballistic Research & Development Center Dover, NJ 07801 (Attn: SMD, Concepts Branch)	4
21. Commanding Officer Army Ballistic Research Laboratories Aberdeen Proving Ground, MD 21005 (Attn: DRDAR-TSB-S (STINFO))	1
22. Headquarters Air Force Systems Command Andrews Air Force Base Washington, DC 20334 (Attn: DLFP, SDW)	2
23. Commanding Officer Air Force Armament Laboratory Eglin Air Force Base, FL 32542 (Attn: DLJW, DLR)	2
24. Commanding Officer Air Force Rocket Propulsion Lab. Edwards AFB, CA 93523 (Attn: MKP)	1
25. Commanding Officer Foreign Technology Division Wright-Patterson AFB, OH 45433 (Attn: Code PDXA, James Woodard, Code XRHP)	2
26. Defense Advanced Research Projects Agency 1400 Wilson Blvd. Arlington, VA 22209	1

	<u>NO. OF COPIES</u>
27. Chairman Department of Defense Explosives Safety Board Room 856-C, Hoffman Bldg. 1 2461 Eisenhower Avenue Alexandria, VA 22331 (Attn: 6-A-145)	1
28. George C. Marshall Space Flight Center Huntsville, AL 35812 (Attn: S&E-ASTN-PJ, Ken Reed)	1
29. Naval Weapon Center China Lake, CA 93555 (Attn: Code 3205)	37
30. Thiokol Corporation, Huntsville Division (Attn: B. B. Stokes) Huntsville, Alabama 35807	1